ISSN 1063-7842, Technical Physics, 2019, Vol. 64, No. 6, pp. 819–827. © Pleiades Publishing, Ltd., 2019.
Russian Text © The Author(s), 2019, published in Zhurnal Tekhnicheskoi Fiziki, 2019, Vol. 89, No. 6, pp. 879–887.

SOLID STATE

Interfacial Stresses and Anomalous Shape of Pseudoelastic Deformation Curves in $Ni_{49}Fe_{18}Ga_{27}Co_6$ Alloy Crystals Compressed along the $[011]_A$ Axis

G. A. Malygin[a,*], V. I. Nikolaev[a], V. M. Krymov[a], S. A. Pul'nev[a], and S. I. Stepanov[a]

[a] *Ioffe Institute, St. Petersburg, 194021 Russia*

**e-mail: malygin.ga@mail.ioffe.ru*

Received October 6, 2018; revised October 6, 2018; accepted November 14, 2018

Abstract—We have performed experimental and theoretical investigation of the anomalous form of the compression diagrams and shape memory restoration curves in $Ni_{49}Fe_{18}Ga_{27}Co_6$ alloy crystals deformed by uniaxial compression along the $[011]_A$ crystallographic direction (*A*-austenite) in the temperature range of 200–350 K. It is found that in the investigated temperature range, all compression diagrams contain anomalous segments of smooth and sharp decrease in deforming stresses. It is shown that the segments of a smooth decrease in stress are associated with peculiarities in martensite reaction $L1_2 \rightarrow 14M$, while segments of a sharp drop are due to instability of martensite reactions $14M \rightarrow L1_0$ and $L1_2 \rightarrow L1_0$. A possible source of reaction instability is associated with interfacial stresses at the interfaces between the martensite and austenite phases (lamellas) due to different elastic moduli of contacting phases. The magnitude of these stresses is significant in the case of $14M \rightarrow L1_0$ and $L1_2 \rightarrow L1_0$ transformations, which induces a sharp drop of the deforming stress, while the restoration of the shape memory effect is of a burst nature. It is established that the contribution of interfacial stresses to the free energy of martensite transformation is smaller than the dissipative (entropy) contribution to this energy; however, interfacial stresses higher than a certain threshold strongly affect transformation kinetics and, hence, determine the strongly anomalous shape of pseudoelastic deformation curves and burst restoration of the shape memory effect.

DOI: 10.1134/S1063784219060124

INTRODUCTION

After the discovery of the magnetic shape memory effect in ferromagnetic Ni_2MnGa alloy [1], alloys of this type have invariably attracted attention of researchers [2–4]. These materials induced interest not only as objects of fundamental theoretical research, but also as promising materials for constructing high-speed technical devices based on the magnetic shape memory effect. Recent experiments on deforming the multicomponent $Ni_{49}Fe_{18}Ga_{27}Co_6$ alloy have revealed several new phenomena that have not been the focus of researchers' interest so far [5–8]. We are speaking of the anomalous shape of pseudoelastic deformation curves of these alloy crystals under uniaxial compression along the $[011]_A$ crystallographic axis. It was found in [5] that pseudoelastic stress–strain curves for this alloy contain two significant segments of deforming stress decay, viz., a smooth (almost from the beginning of straining) decrease and a sharp drop at the end of the compression diagram. Since compression diagrams of a Ni–Fe–Ga–Co crystal compressed in the direction of the $[001]_A$ axis usually have the shape of monotonically ascending curves [5, 6], the presence of anomalous stress decays under its compression along the [011] axis indicates anisotropy in deformation properties of the crystal. It should be noted above all that such anomalies on stress–strain diagrams were also observed for other crystals with the shape memory effect (SME). Such anomalies were detected, for example, during the compression of Cu–Al–Ni alloy single crystals along the [001] direction [9–11]. The recovery of this deformation under reverse martensite transformation also occurs unusually in the ultrasonic temperature interval ($\sim 10^{-3}$ K) [5, 6, 12].

This is manifested visually in the fact that a crystal resting on a solid support and heated at a constant rate jumps above the support due to its response to a height of about 20 m at a velocity of separation of the crystal from the support exceeding 20 m/s. However, the rate of shape restoration of the crystal deformed in the direction of the $[001]_A$ axis does not exceed 20 μm/s and develops in the temperature interval of about 4 K. Analysis based on preset partial shape memory strains shows [12] that the burst restoration of shape memory in alloy crystals is associated with the second (sharp) decrease of stress on the compression diagram of this

crystal deformed along the $[011]_A$ axis. These peculiarities of $Ni_{49}Fe_{18}Ga_{27}Co_6$ alloy crystals were considered in [7, 8].

The available data on deformation by compression of the $Ni_{54}Fe_{19}Ga_{27}$ alloy with close composition show [13, 14] that the stress–strain diagram for compression in the $[011]_A$ direction has a normal form. Diagrams for compression of ternary and four-component alloys along the $[001]_A$ axis behave analogously, i.e., have a form typical of σ–ε diagrams with smoothly increasing deforming stress σ [5, 6, 14]. It was proposed in [7] that the emergence of two stress decay segments on the pseudoelastic deformation curve for a Ni–Fe–Ga–Co alloy compressed along the $[011]_A$ axis and the burst-like form of shape memory strain restoration in this alloy are due to the fact that the presence of 6 at % Co in the alloy leads to a strong increase in the interfacial stress level and induces instability of the following martensite transformations: fcc austenite $L2_1 \rightarrow$ modulated (twinned) 14M martensite $\rightarrow$ tetragonal $L1_0$ martensite.

This article is aimed at detailed analysis of anomalies on pseudoelastic deformation curves and subsequent high-speed (burst) restoration of the shape memory strain in $Ni_{49}Fe_{18}Ga_{27}Co_6$ crystals in the temperature range from 200 to 350 K. These effects have not been studied so far in such a wide temperature interval, and the level of interfacial stresses in this alloy and its influence on the kinetics and deformation energy parameters of the alloy have not been determined experimentally. The theoretical foundation of analysis of the observed strain anomalies is the theory of diffuse martensitic transformations [15, 16].

1. EXPERIMENTAL

Samples of $Ni_{49}Fe_{18}Ga_{27}Co_6$ crystals 4 × 4 × 9 mm in size with [011] orientation in the austenite phase were cut on an electrospark discharge machine, held at a temperature of 1423 K for 1 h in evacuated quartz ampoules, and quenched in water. The phase state of initial quenched crystals was determined using a Mettler-DSC822e differential calorimeter at a temperature scanning rate of 10 K/min.

The crystal was compressed in an Istron 1342 testing machine at a strain rate of 5×10^{-4} s^{-1} at eight different temperatures in the range 200–350 K. After unloading, crystals were placed into a special setup for measuring the rate of shape memory strain restoration [17, 18], in which samples were heated at a constant rate of 1–2 K/min. Shape restoration rate V of the crystal in the range 10^{-6}–10^{-4} m/s was determined using a laser interferometer. At high rates, video recording was used for estimating the temperature at which crystal shape restoration becomes unstable (burst-like), and the crystal leaps up above the support due to its response. To match the velocity of crystal separation from the support with temporal and spatial resolution limits of the video camera, the sample being heated was loaded by an additional weight with a mass of 690 g. The velocity of crystal separation from the support was calculated from the results of video recording that fixed the maximal lifting height H of the sample with a load. Velocity V_0' of separation of the sample–weight system was determined from its maximal lift height as $V_0' = (2gH)^{1/2}$. The velocity of the sample without a load was calculated by formula $V_0 = (1 + M/m)^{1/2}V_0'$, where $m = 1.0$ g is the crystal mass and M is the mass of extra weight. In calculating V_0, we assumed that the entire volume of the crystal is involved in burst-like martensitic transformation.

1.1. Compression Diagrams

Figure 1 shows the diagrams of compression of $Ni_{49}Fe_{18}Ga_{27}Co_6$ alloy crystals in the direction of the $[011]_A$ axis at eight temperatures from the interval 200–350 K. Their peculiarity lies in two descending segments of deforming stress, one smooth in a strain interval of 2–4% and another sharp in the strain interval of 4–6%, as well as a segment of elastic increase of stress between these segments. As noted above, the compression diagrams of this alloy crystal in the $[001]_A$ direction have a conventional shape (increase monotonically with strain) and are of a one-stage form [5, 6]. In the absence of Co, compression diagrams of ternary alloy $Ni_{54}Fe_{18}Ga_{27}$ in the [001] and [011] directions also have a conventional (ascending) form according to [13, 14]. These diagrams have one stage for straining along the [001] direction and two stages for compression along the [011] axis.

The two-stage nature of direct and reverse martensitic transformations in the $Ni_{49}Fe_{18}Ga_{27}Co_6$ alloy also follows from the calorimetric data shown in Fig. 2. Relatively broad peak M_1 recorded under cooling can be identified as the $L2_1 \rightarrow 14M$ transformation, while narrower peak M_2 can be attributed to the $14M \rightarrow L1_0$ transformation, where 14M is twinned and $L1_0$ is untwinned tetragonal martensite. During heating, the reverse sequence of transformations is observed. The final result is the transformation of tetragonal martensite into fcc austenite. The values of heat q and temperatures of direct ($M_{s,f}$) and reverse ($A_{s,f}$) transformations, as well as characteristic temperatures T_c corresponding to peaks on the curves for heat release and absorption in the crystal during phase transformations are given in Table 1. The total heat of two-stage martensitic transformation is 4.69 J/g for cooling and 4.56 J/g for heating, which indicates a high reversibility of the given martensitic transformation.

For analyzing the experimental diagrams in Fig. 1, we chose the following characteristic parameters of σ–ε curves, which are shown schematically in Fig. 3:

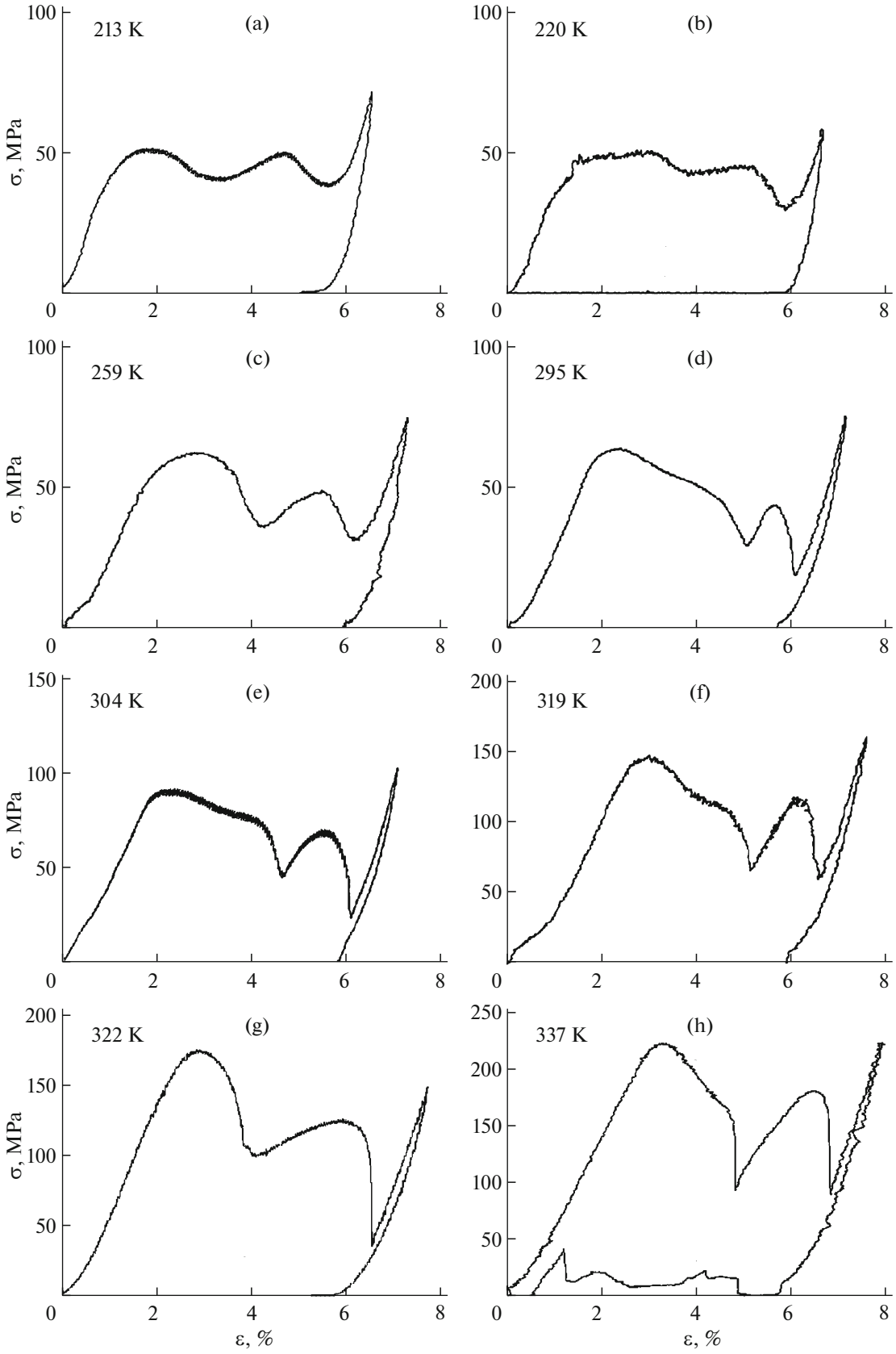

Fig. 1. Diagram of compression of $Ni_{49}Fe_{18}Ga_{27}Co_6$ alloy single crystals in the direction of the $[011]_A$ crystallographic axis at temperatures 213–337 K.

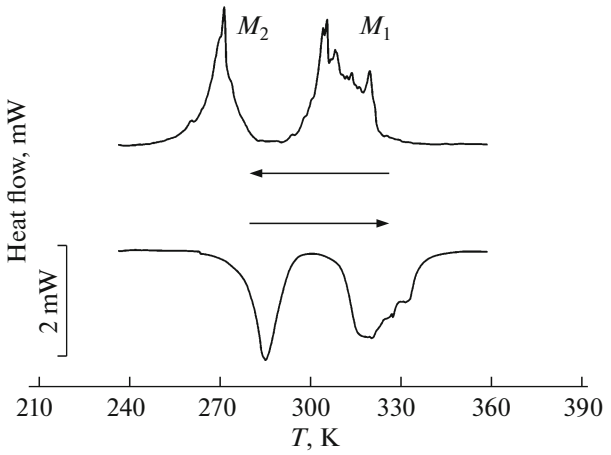

Fig. 2. Calorimetric curves for $Ni_{49}Fe_{18}Ga_{27}Co_6$ alloy crystals for direct and reverse martensitic transformations.

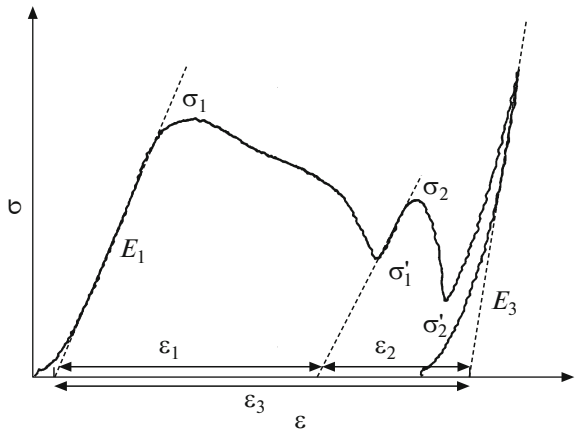

Fig. 3. Diagram for calculating elastic moduli E_u, ultimate stresses σ_u and σ'_i, and strains ε_i of the σ–ε diagrams shown in Fig. 1.

local maxima σ_i and minima σ'_i of stresses, strains ε_i on the characteristic segment of stress decay ε_i, and elastic moduli E_i. Figure 4 shows the dependence of these moduli on characteristic segments of the diagram on temperature T_d of crystal compression. Modulus E_1 in the temperature interval up to about 295 J has an average value of about 3.2 GPa and corresponds to homogenization of variants of martensite 14M, and above 295 K, it corresponds to elastic modulus $E_{14M} \approx$ 6 GPa of its homogenized variant. Modulus E_2 (filled triangles) at temperatures above 295 K also tends to this value. Elastic modulus E_3 for unloading (filled squares) characterizes the elasticity of tetragonal $L1_0$ martensite, $E_{L1_0} \approx 14$ GPa, and is almost independent of the temperature of crystal compression. Figure 4 also shows the dependences of strains ε_1 and ε_2 corresponding to the first and second stages of pseudoelastic deformation of the alloy, as well as its strain $\varepsilon_3 \approx$ 6.2% during unloading, on temperature T_d. It can be seen that strain ε_3 is almost independent of the compression temperature, while the strain at the first stage (filled circles) increases with temperature. At temperatures higher than 295 K, the strain approaches a value of about 4%, while the strain at the second stage (triangles), conversely, decreases from this value and tends to about 2%.

Table 1. Parameters of martensitic transformations in $Ni_{49}Fe_{18}Ga_{27}Co_6$ alloy according to differential scanning calorimetry data

Parameters	$L2_1 \rightarrow 14M$	$14M \rightarrow Ll_0$
q, J/q	3.02*/–2.59**	1.67*/–1.97**
T_c, K	307*/312**	268*/284**
M_s, K	322	278
M_f, K	299	262
A_s, K	309	277
A_f, K	336	293

* Corresponds to cooling and ** to heating.

Figure 5 shows the temperature dependences of stresses σ_1 and σ_2 corresponding to maximal stresses at the first (filled circles) and second (triangles) stages of compression diagrams in Fig. 1. These dependences are weak up to a temperature of 295 K and become substantially stronger above this temperature. For stress σ_1, the slope of dashed curve *1* corresponds to Clausius–Clapeyron coefficient $d\sigma/dT = 4$ MPa/K, while for stress σ_2, it corresponds to coefficient 3.3 MPa/K. According to [14], coefficient 4 MPa/K for ternary alloy $Ni_{54}Fe_{19}Ga_{27}$ corresponds to the reaction of formation of 14M martensite under compression of samples of this alloy along the [011] axis at temperatures above 295 K, while coefficient 2.6 MPa/K at temperatures above 317 K corresponds to martensitic reaction $L2_1 \rightarrow L1_0$ (i.e., to the direct transformation of austenite into tetragonal martensite). In the case of the $Ni_{49}Fe_{18}Ga_{27}Co_6$ alloy, this coefficient (dot-and-dash curve *2*) has a higher value of 3.3 MPa/K.

If we assume that the stress drops on pseudoelastic deformation curves in Fig. 1 are due to relaxation of interfacial stresses [7], the values of these stresses can be estimated in the first approximation as difference of stresses $\sigma_1 - \sigma'_1$ and $\sigma_2 - \sigma'_2$ at the first and second stages of pseudoelastic deformation curves, respectively (see diagram in Fig. 3). The dependence of these differences on crystal compression temperature of the crystal is shown in Fig. 6. It can be seen that these differences are relatively small up to 295 K. Above this temperature, the differences strongly increase and are stabilized at a level of about 90 MPa at temperatures above 317 K. According to [14], temperatures of 295 and 317 K correspond to the beginning of twinning of

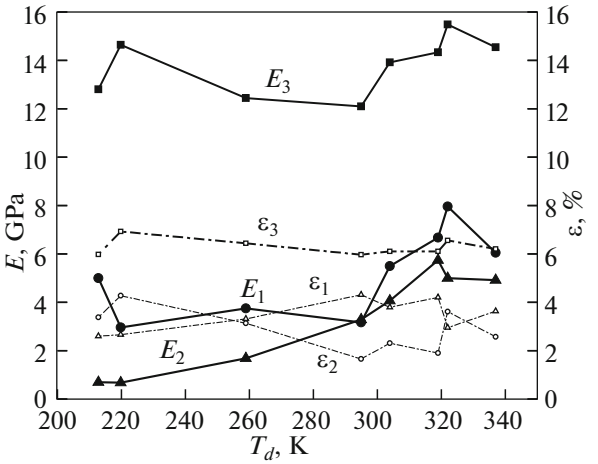

Fig. 4. Dependences of elastic moduli E_1, E_2, and E_3 and strains ε_1, ε_2, and ε_3 on three segments of the σ–ε diagram on temperature T_d of compression deformation of crystals.

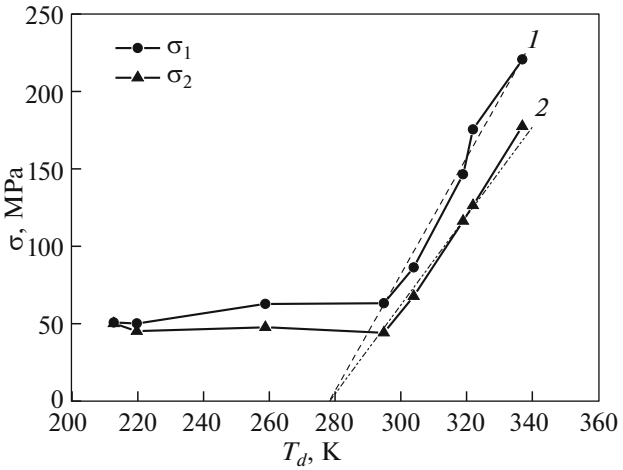

Fig. 5. Dependences of local maxima of stresses σ_1 and σ_2 on temperature T_d of compression deformation of crystals.

$L1_0$ martensite and direct transformation of austenite into $L1_0$ martensite in crystals of a Ni–Fe–Ga alloy under its compression in the $[110]_A$ direction. The low level of interfacial stresses up to 295 K is obviously due to low values for the $L2_1 \rightarrow 14M$ transformation. At temperatures above 295 K, $L1_0$ martensite becomes heterophase as a result of twinning, which elevates the level of interfacial stresses in it. For direct transformation of austenite into $L1_0$ martensite, interfacial stresses attain their maximal values beginning from 317 K.

It would also be interesting to analyze the energy parameters of these transformations upon an increase in the crystal compression temperature. Figure 7 shows the results of integration over strain ε (see Fig. 1) of the entire compression diagram (A_3) and its first (A_1) and second (A_2) stages separately. The results of integration are given in joules per gram. It can be seen that up to a straining temperature of 295 K, the work done for deforming the alloy is almost independent of the compression temperature, while above 295 K, it rapidly increases with this temperature. Straight lines *1*–*3* in Fig. 7 above 295 K have slopes of 2.6, 2.33, and 4.6 J/g, respectively. These values should be compared with the values of energy q in Table 1, which were obtained from the processing of the calorimetric data for this alloy. The value of energy (enthalpy) of complete $L2_1 \rightarrow 14M \rightarrow L1_0$ martensitic transformation under a stress of 4.6 J/g agrees with total specific energy $q = q_{14m} + q_{L1_0} = 4.56$–$4.69$ J/g of direct and reverse transformations (see Table 1). Temperatures of 277 and 283/284 K (extrapolation of the dotted line to the temperature axis) correspond to the characteristic temperatures of direct and reverse $14M \rightarrow L1_0$ transformations given in Table 1. Regarding A_1 and A_2 spent for formation of 14M martensite in the temperature range up to 295 K, the averaged value of these quantities is 0.19 J/g.

1.2. Burst Restoration of Crystal Shape

The experiments on preset shape memory strains at room temperature show [12] that the effect of burst realization of shape memory deformation in $Ni_{49}Fe_{18}Ga_{27}Co_6$ crystals deformed by compression in the direction of the $[011]_A$ axis is observed only after setting strains corresponding to the second decay of stress on pseudoelastic deformation curves. Figure 8 shows the dependence of initial velocity V_0 of elevation of a crystal above the support from temperature T_{bst} at which burst restoration of the shape memory strain

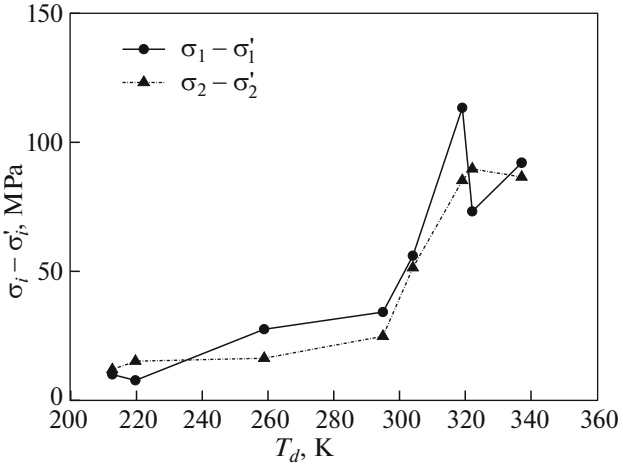

Fig. 6. Dependences of the difference in the stresses corresponding to the maxima and minima on the compression curves for the crystals on temperature T_d of compression deformation in accordance with the diagram in Fig. 3

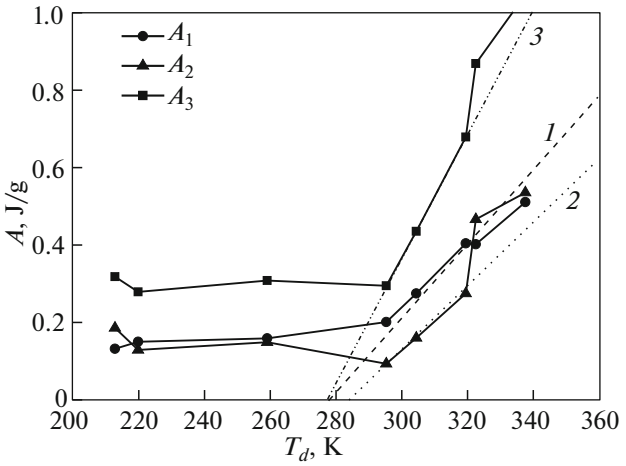

Fig. 7. Dependences of the work for compression of $Ni_{49}Fe_{18}Ga_{27}Co_6$ alloy crystals at the first (A_1) and second (A_2) stages of the pseudoelastic deformation curves and their sum on temperature T_d of compression deformation of crystals.

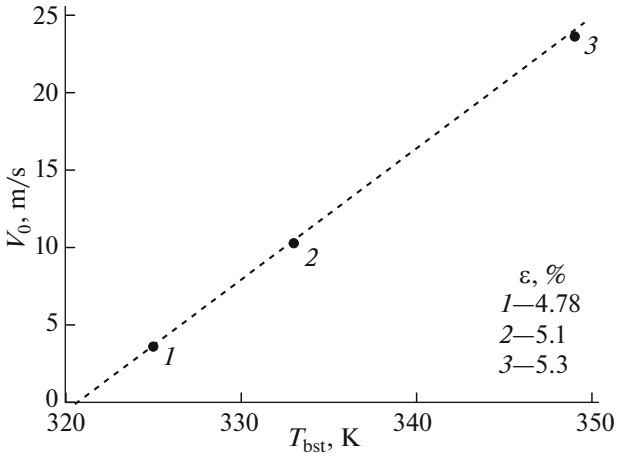

Fig. 8. Parametric dependences of the relative velocity of crystal detachment from the support in temperature interval 270–330 K for three values of relative interfacial stresses $a = \sigma_e/\sigma_m$: a = 0 (*1*), 0.17 (*2*), and 0.4 (*3*). The scale of relative velocities of detachment of the crystal from the support for lines *1* and *2* is magnified tenfold.

occurred upon heating. The sample was deformed up to three values of particle shape memory strain indicated in Fig. 8. At partial strains (smaller than 4.8%), the motion of the sample during the bounce from the support was not manifested clearly, its jitter on the support was observed, which was associated with sequential small steps of shape memory strain restoration.

In this study, the effect of burst restoration of shape memory deformation in $Ni_{49}Fe_{18}Ga_{27}Co_6$ crystals is studied in a wide range of temperatures T_d of preliminary compression of a crystal. Figure 9 shows the dependence of the velocity of detachment of a crystal from a solid support on the compression temperature. It can be seen from the data in Fig. 9 that burst-like restoration of the crystal shape was observed at all investigated temperatures. Up to 295 K, the velocity of detachment was almost independent of temperature T_d (line *1*), while above this temperature, this velocity noticeably increases with temperature (line *2*).

2. DISCUSSION OF RESULTS

The above results of experiments on compression of $Ni_{49}Fe_{18}Ga_{27}Co_6$ alloy crystals along the $[011]_A$ axis and burst recovery of shape memory strain in them indicate a peculiar evolution of martensitic transformations in the crystals in question. It was proposed in [7] that the reason for the peculiar shape of pseudodeformation curves for the alloy doped with 6 at % Co are interfacial stresses. Their magnitude depends to a considerable extent on crystal orientation relative to its compression axis as well as on the form of martensitic reaction. Interfacial stresses are higher for martensitic reactions 14M $\rightarrow$ $L1_0$ and $L2_1$ $\rightarrow$ $L1_0$ and are noticeably lower for the $L2_1$ $\rightarrow$ 14M reaction; twinning appreciably reduces the value of these stresses in 14M martensite.

Available data on the effect of concentrations of Co atoms exceeding 3 at % on parameters of martensitic transformations in Ni–Fe–Ga–Co alloy crystals can be described as follows. An increase in the cobalt con-

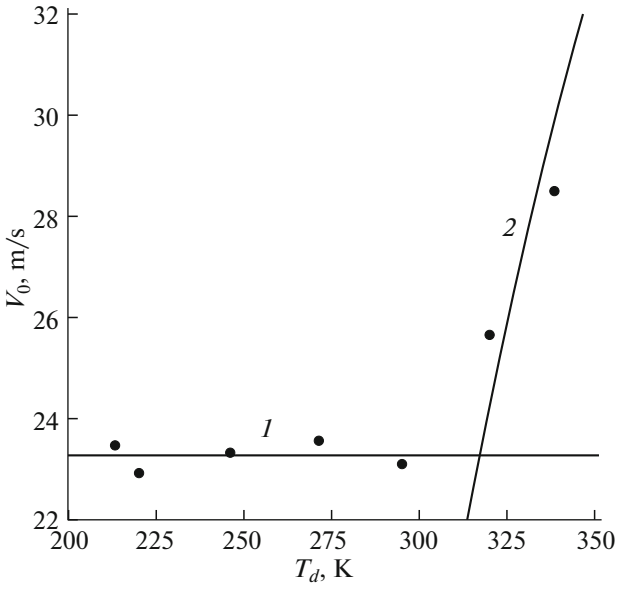

Fig. 9. Dependence of the initial velocity of detachment of the $Ni_{49}Fe_{18}Ga_{27}Co_6$ alloy crystal from the support on temperature T_{bst} of the burst-like martensitic transformation for three values of compressive strain indicated in Fig. 8, corresponding to the second stage of the pseudoelastic deformation curve for the alloy at T_d = 293 K.

centration in the alloy by substitution of Ni or Fe atoms induces a shift in martensitic transformation temperatures towards their increase [4] and also increases the Curie temperature and magnetic anisotropy of the alloy [2]. It has been established that cobalt also leads to deformation anisotropy under compression of $Ni_{49}Fe_{18}Ga_{27}Co_6$ crystals along the [001] and [011] axes [5], which is not observed for the $Ni_{54}Fe_{19}Ga_{27}$ alloy [13, 14]. According to [2–4], Co atoms induce an increase in the lattice tetragonality, which is accompanied by additional structural deformations and, hence, with the emergence of interfacial stresses in the alloy.

According to the theory of diffuse martensitic transformations (DMTs), relative crystal volume φ_M occupied by martensite with temperature T and stress σ in the one-stage martensitic transformation is given by

$$\varphi_M = \frac{1}{1+\exp(\Delta U/kT)}, \quad (1a)$$

where $\Delta U = \omega\Delta u$ is the change in the free energy of the alloy due to the formation of a new phase nucleus of volume ω in it, Δu is the volume density of free energy of the phase transition,

$$\Delta u = q\frac{T-T_c}{T_c} - \varepsilon_m\sigma + W_{el}, \quad (1b)$$

where q is the heat of transition, ε_m is the lattice strain in its structural rearrangement, T_c is the characteristic temperature of transformation, k is the Boltzmann constant, $W_{el} = \sigma_e\varepsilon_M(\varphi_M)$ is the elastic energy associated with phase transition,

$$\varepsilon_M(\varphi_M) = \varepsilon_m\varphi_M(1-\varphi_M), \quad (1c)$$

where ε_M are interfacial strains, σ_e is the interfacial stress, and ε_m is the strain of the martensitic transformation. Equations (1a)–(1c) describe the equilibrium of austenite and martensite phases in a crystal depending on temperature, stress, and interfacial stresses. Equation (1c) implies that in one-phase states, where $\varphi_M = 0$ (austenite) and $\varphi_M = 1$ (martensite), interfacial strains and interfacial energy

$$W_{el}(\varphi_M) = \sigma_e\varepsilon_m\varphi_M(1-\varphi_M) \quad (2)$$

vanish, while for $\varphi_M = 1/2$, these quantities attain their maximal values. The value of interfacial stresses σ_e depends on the assumption concerning their sources. This can be the difference between the elastic moduli of austenite and martensite phases in form $\sigma_e = (E_M - E_A)\varepsilon_m$ [12] or the difference in elastic energies of the phases, $W_{el} = [(E_M - E_A)/2E_ME_A]\sigma^2$, where σ is the stress applied to the crystal. In the former case, it is assumed that interfacial stresses exist even in the absence of an external stress applied to the crystal; in the latter case, it is assumed that these stresses are generated by it. Here, we consider only the former assumption.

Substituting Eq. (2) into (1b) and (1b) into (1a) and solving the latter equation for stress σ, we obtain its dependence on temperature, interfacial stresses, and martensitic strain $\varepsilon = \varepsilon_m\varphi_M$ of a crystal:

$$\sigma = \sigma_m\left[\frac{T-T_c}{T_c} - a\frac{\varepsilon}{\varepsilon_m}\left(1-\frac{\varepsilon}{\varepsilon_m}\right) + \frac{kT}{\omega q}\ln\left(\frac{\varepsilon/\varepsilon_m}{1-\varepsilon/\varepsilon_m}\right)\right], \quad (3a)$$

where $\sigma_m = q/\varepsilon_m$ and $a = \sigma_e/\sigma_m$. Equation (3a) implies that for a certain value of parameter a, which determines the relative value of interfacial stresses σ_e, martensite strain-hardening coefficient $\theta = d\sigma/d\varepsilon$, which is given by

$$\theta = \left(\frac{kT}{\omega\varepsilon_m^2}\right)\frac{1}{(1-\varepsilon/\varepsilon_m)\varepsilon/\varepsilon_m} - \sigma_e(1-2\varepsilon/\varepsilon_m) \quad (3b)$$

may become negative, which means that a segment with decreasing stress appears on the compression diagram.

Work A done by the external force for compressing a crystal from zero to ultimate martensite strain ε_m is given (in accordance with relation (3a)) by

$$A(T,\sigma_e) = \int_0^{\varepsilon_m}\sigma d\varepsilon = q\frac{T-T_c}{T_c} - \frac{1}{6}\sigma_e\varepsilon_m. \quad (4)$$

It contains two parts, dissipative and elastic, which is associated with interfacial stresses σ_e. In accordance with Eq. (4), interfacial stresses reduce the work done on deforming a crystal by $A_e = \sigma_e\varepsilon_m/6$. The dissipative part of the study is independent of crystal orientation and is determined by the temperature and heat of the martensitic transformation per unit mass of the crystal. According to results shown in Fig. 7, the interfacial stress in the studied crystal at 288 K amount to approximately 30 MPa, while the martensitic transformation strain is $\varepsilon_m = \varepsilon_2 \approx 2\%$ (see Fig. 4). Substituting these values into relation $A_e = \sigma_e\varepsilon_m/6$ and considering that in this alloy the specific density of about 9×10^6 g/m^3 is equivalent to 9 J/m^3 (i.e., 9 MPa), we obtain an estimate on the order of 0.01 J/g for contribution A_e of interfacial stresses to the total work of compression of a crystal of the given alloy. According to the results depicted in Fig. 7, the work done for sample compression at room temperature is $A_2 \approx 0.2$ J/g, i.e., is an order of magnitude higher. The absence of an appreciable effect of interfacial stresses on the energy parameters of martensite deformation indicates that interfacial stresses mainly affect kinetics of martensitic transformation, as a result of which segments of an anomalous drop of the deforming stress are observed on compression diagrams of crystals with the shape memory effect (see Fig. 1).

This also follows from the anomalous burst-like form of the restoration of crystal shape upon its heating after compression. During heating, the height of a compression-deformed crystal resting on a solid support increases in accordance with relation $h = (1 -$

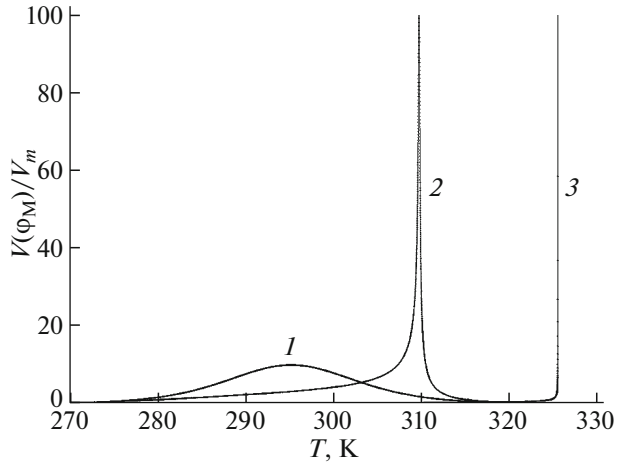

Fig. 10. Dependences of the velocity of detachment of the crystal from the support on temperature T_d of compression deformation of crystals for total shape memory strain. Circles correspond to experiment and curves *1* and *2* are calculated theoretically.

$\varepsilon_m\varphi_M)h_0$ upon a transformation of martensite into austenite, where h_0 is the initial height prior to deformation. The rate of shape recovery of the crystal heated at constant rate $\dot{T}$,

$$V = dh/dt = h_0 d(\varepsilon_m\varphi_M)dt = h_0\varepsilon_m\dot{T}d\varphi_M/dT, \quad (5a)$$

is determined by the rate of martensitic transformation $\dot{T}\,d\varphi_M/dT$. Differentiating relation (1a) with respect to temperature at $\sigma = 0$ and considering the interfacial stresses, we obtain the temperature dependence of the shape (height) recovery rate for a crystal:

$$V(\varphi) = V_m\frac{4\varphi(1-\varphi)}{1-a\bar{\omega}\varphi(1-\varphi)(1-2\varphi)}, \qquad V_m = \frac{\bar{\omega}\varepsilon_m h_0}{4T_c}\dot{T}, \quad (5b)$$

where $\bar{\omega} = \omega q/kT$, $a\bar{\omega} = \sigma_e\varepsilon_m\omega/kT_c$, $V_m \approx 20$ μm/s is the maximal rate of crystal shape restoration for $\varphi = 1/2$ and a stable form of transformation [5] (i.e., in the absence of interfacial stresses, $a = 0$). The curves in Fig. 10 demonstrate temperature dependences of relative rate $V(\varphi)/V_m$ of crystal shape restoration,

$$T(\varphi) = T_c\left[1 + a\varphi(1-\varphi) - \frac{1}{\bar{\omega}}\ln\left(\frac{\varphi}{1-\varphi}\right)\right] \quad (6)$$

for three values of parameter $a = \sigma_e/\sigma_m$: $a = 0$ (*1*), 0.17 (*2*), and 0.4 (*3*) at $T_c = 295$ K and $\bar{\omega} = 60$. In accordance with relation (3), temperature is parametrically connected with relation (5b) for $\sigma = 0$ in terms of φ. In the absence of interfacial stresses, the denominator of formula (5b) is independent of temperature $T(\varphi)$. When parameter $a = 0.17$, it vanishes at temperature 310 K, and the crystal shape restoration rate turns to infinity (curve *2* in Fig. 10). This means that the martensitic transformation loses stability at temperature 310 K. For values of parameter a higher than 0.17, instability is manifested at a higher temperature (curve *3* in Fig. 10). With increasing temperature $T_{bst} = T(\varphi_{bst})$ of martensitic transformation stability loss, the velocity of crystal detachment from the support increases (see Fig. 8).

The results shown in Fig. 7 (curves *1*, *2*) show that the work of compression of a crystal of mass 1.0 g at room temperature is $W \approx 0.2$ J. Assuming that in the case of reverse martensitic transformation this stored energy is converted into kinetic energy $(1/2)mV_0^2$ of the crystal leap during its detachment from the support, we obtain estimate $V_0 = (2W/m)^{1/2} = (2A)^{1/2}$ for the initial velocity of the leap, where A is the energy per unit mass of the crystal. Considering further that 1 J/g is equivalent to 10^3 m^2/s^2, energy $A = 0.2$ J/g is sufficient for imparting an initial velocity of 20 m/s to a crystal and to raise it to height $H = V_0^2/2g = A/g \approx 20$ m, where g is the acceleration due to gravity. Curve *1* in Fig. 9 demonstrates the calculated dependence of velocity V_0 on temperature T_d of crystal compression not higher than 295 K in the case when energy A, according to the results shown in Fig. 7, is almost independent of the temperature of crystal compression. Curve *2* in Fig. 9 demonstrates the dependence of velocity $V_0 = (2A_2(T_d))^{1/2}$ for energy A_2 approximated by equation $A_2(T_d) = 2.33(T_d/284 - 1)$ (curve *2* in Fig. 7).

CONCLUSIONS

Analysis of the role of interfacial stresses in the emergence of anomalies on pseudoelastic deformation curves and shape memory strain recovery in $Ni_{49}Fe_{18}Ga_{27}Co_6$ alloy crystals leads to the following conclusions.

1. Such anomalies are observed in a wide temperature range in the emergence of noticeable decrease in stresses on the pseudoelastic deformation curves followed by burst-like restoration of the shape memory strain in these alloy crystals compressed along the $[011]_A$ axis.

2. The most probable reason for these anomalies is interfacial stresses emerging due to the difference in elastic moduli of the martensite and austenite phases.

3. The interfacial stresses are relatively small for the $L2_1 \rightarrow 14M$ martensitic transformation and large for $14M \rightarrow L1_0$ and $L2_1 \rightarrow L1_0$ transformations.

4. Interfacial stresses do not significantly affect the energy parameters of martensitic transformations, but strongly influence their kinetics. As a result, martensitic transformations become unstable, which determines the anomalous shape of pseudoelastic deformation curves and the burst-like restoration of the shape memory strain.

FUNDING

This work was supported by the Russian Science Foundation (project no. 16-19-00129)

REFERENCES

1. K. Ullakko, J. K. Xuang, C. Kantner, R. C. O'Handley, and V. V. Kokorin, Appl. Phys. Lett. **69**, 1966 (1996).
2. H. Morito, K. Oikawa, A. Fujita, K. Ishida, K. Fukamichi, and R. Kainuma, Appl. Phys. Lett. **90**, 062505 (2007).
3. H. Morito, A. Fujita, K. Oikawa, K. Fukamichi, R. Kainuma, K. Ishida, and T. Takagi, J. Magn. Magn. Mater. **290–291**, 850 (2005).
4. H. Zheng, M. Xia, J. Liu, Ya. Huang, and J. Li, Acta Mater. **53**, 5125 (2005).
5. V. I. Nikolaev, P. N. Yakushev, G. A. Malygin, and S. A. Pul'nev, Tech. Phys. Lett. **36**, 914 (2010).
6. V. I. Nikolaev, G. A. Malygin, S. A. Pulnev, P. N. Yakushev, and V. M. Egorov, Mater. Sci. Forum **738–739**, 51 (2013).
7. G. A. Malygin, V. I. Nikolaev, A. I. Averkin, and A. P. Zograf, Phys. Solid State **58**, 2488 (2016).
8. V. I. Nikolaev, G. A. Malygin, A. I. Averkin, S. I. Stepanov, and A. P. Zograf, Mater. Today: Proc. **4**, 4807 (2017).
9. C. Picornell, J. Pons, and E. Cesari, Mater. Sci. Eng., A **378**, 222 (2004).
10. A. Ibarra, J. San Juan, E. H. Bocanegra, and M. L. No, Acta Mater. **55**, 4789 (2007).
11. V. I. Nikolaev, P. N. Yakushev, G. A. Malygin, A. I. Averkin, A. V. Chikiryaka, and S. A. Pul'nev, Tech. Phys. Lett. **40**, 123 (2014).
12. V. I. Nikolaev, P. N. Yakushev, G. A. Malygin, A. I. Averkin, S. A. Pul'nev, G. P. Zograf, S. B. Kustov, and Yu. I. Chumlyakov, Tech. Phys. Lett. **42**, 399 (2016).
13. E. Panchenko, Yu. Chumlyakov, H. J. Maier, E. Timofeeva, and I. Karaman, Intermetallics **18**, 2458 (2010).
14. E. E. Timofeeva, E. Yu. Panchenko, Yu. I. Chumlyakov, and H. Maier, Russ. Phys. J. **54**, 1427 (2012).
15. G. A. Malygin, Phys.-Usp. **44**, 173 (2001).
16. G. A. Malygin, Phys. Solid State **43**, 1339 (2001).
17. P. N. Yakushev, Opt. Mem. Neural Networks **18**, 222 (2004).
18. N. N. Peschanskaya, V. V. Shpeizman, P. N. Yakushev, A. S. Smolyanskii, and A. S. Shvedov, Bull. Russ. Acad. Sci.: Phys. **73**, 1427 (2009).

Translated by N. Wadhwa